Journal of Materials Processing Technology 209 (2009) 4548–4552

Contents lists available at ScienceDirect

Journal of Materials Processing Technology

journal homepage: www.elsevier.com/locate/jmatprotec

Cutting composites: A discussion on mechanics modelling

L.C. Zhang*

School of Aerospace, Mechanical and Mechatronic Engineering, The University of Sydney, NSW 2006, Australia

ARTICLE INFO

Article history:
Accepted 6 October 2008

Keywords:
Cutting
Composites
Modelling
Long fibre
Metal matrix
Ceramic particle

ABSTRACT

Using the cutting of long fibre reinforced polymer and ceramic particle reinforced aluminium as the examples, this paper tends to understand some common features in the mechanics modelling of machining composites. It demonstrates that an accurate characterisation of matrix deformation, matrix–reinforcement interaction, and reinforcement deformation are key factors for the establishment of a model to reflect the principal material removal mechanisms. A precise understanding of these factors can be achieved through a logic process of mechanism exploration, model derivation and verification.

© 2008 Elsevier B.V. All rights reserved.

1. Introduction

Composites have been extensively used in a wide range of technical fields, such as in the automotive industry for making engine-connecting rods, propeller shafts, brake discs and, in the leisure industry for fabricating tennis racquets. There are many sorts of composites for specific applications, but some commonly used are the long fibre reinforced polymer matrix composites (LFRCs) and ceramic particle/fibre reinforced metal matrix composites (MMCs). Usually, a composite contains high hardness or high strength reinforcements, causing a significant problem for machining, because cutting tools wear severely, resulting in low accuracy and high machining cost. Meanwhile, due to the very different mechanical properties of the matrix and reinforcement materials, the surface integrity of a machined composite is hard to control, including surface roughness, residual stresses and subsurface damages.

In the past decades, the problems associated with precision and efficiency in cutting composites have become important issues in the manufacturing industry. Investigations into the machining mechanisms and production cost, such as those related to tool wear, selection of machining parameters, and control of surface finish, have been carried out. For example, Wang and Zhang (1999) investigated the cutting of long fibre reinforced composites and found that the machinability and surface integrity are mainly governed by the fibre-orientation relative to the cutting direction. König et al. (1985) reviewed some problems in machining LFRCs. Zhang et al. (2001a,b) discussed the assessment and characterisation of the exit defects in drilling LFRCs and offered some empirical formulae for predicting the spalling size in drilling. Wang et al. (1995) studied the effects of tool geometry and fibre-orientation. Bhatnagar et al. (1995) used a shear test to evaluate the in-plane shear strength of LFRC specimens and proposed a model for the prediction of cutting forces. Arola and Ramulu (1997) and Mahdi and Zhang (2001) applied the finite element method to investigate the cutting of LFRCs. The former adopted a homogenized material model, while the latter considered the micro-details of individual fibre–tool interactions and simulated the breaking process of a single fibre during cutting.

Several force prediction models have also been developed for cutting MMCs. For instance, Kishawy et al. (2004) developed an energy-based analytical model to predict the forces in orthogonal cutting of an MMC using a ceramic tool at a low cutting speed. Pramanik et al. (2006) established a mechanics model for predicting the forces of cutting ceramic particle reinforced MMCs based on the force generation mechanisms of chip formation, matrix ploughing, and particle fracture/displacement.

Although the methods used in studying the machining of composites have been diverse, the investigations can be generally divided into three categories: experimental study focusing on the macro/microscopic machinability of composites, simple modelling using conventional cutting mechanics, and numerical simulations that treat a composite as a macroscopically anisotropic material or concentrate on the reinforcement–matrix interaction microscopically. The macroscopic models normally ignore many fundamental characteristics of composites subjected to cutting and usually cannot be well integrated with the cutting mechanics, while those focusing on the micro-effects, including the analysis using the finite element method, cannot offer practical formulae for direct applications. A sensible way seems to combine the merits of these

* Tel.: +61 2 9351 2835; fax: +61 2 9351 7060.
E-mail address: L.Zhang@usyd.edu.au.

0924-0136/$ – see front matter © 2008 Elsevier B.V. All rights reserved.
doi:10.1016/j.jmatprotec.2008.10.023

methods to develop realistic models that not only depict the material removal mechanisms in cutting, but also provide simple, analytical solutions for applications.

This paper tends to understand some common features of such modelling through a discussion on two mechanics modelling processes for predicting the forces in cutting LFRCs and MMCs. It is expected that this will provide a useful guideline for modelling more complex machining of composites.

2. Cutting of LFRCs

2.1. Mechanism understanding

Experimentally, Wang and Zhang (1999) and Zhang et al. (2001a,b) have found that the fibre-orientation in an LFRC relative to the direction of cutting, θ, is a key factor that determines the cutting forces and the surface integrity of a machined component. As shown in Fig. 1, $\theta = 90^\circ$ is a critical angle, beyond which severe subsurface damages will occur, surface roughness will increase remarkably and the deformation mechanisms in the cutting zone will change.

Zhang et al. (2001a,b) pointed out that there are three distinct deformation regions in the cutting zone, as denoted in Fig. 2, when the fibre-orientation θ varies between 0° and 90°. The first region is in front of the rake face of the cutting tool, resulting in a chip, called a *Chipping Region* or *Region 1*. Fracture occurs at the cross-sections of the fibres and along the fibre–matrix interfaces. The chipping along an overall shear plane, as shown in the figure, is the result of a zigzag cracking of the fibres perpendicular to the fibre axes and

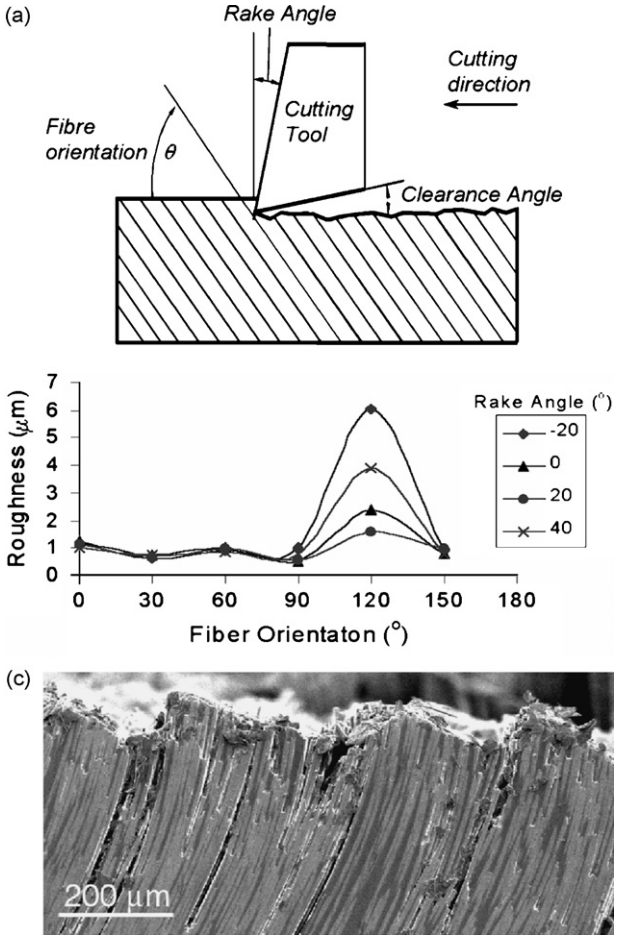

Fig. 1. Cutting of LFRCs. (a) A schematic of the orthogonal cutting of an LFRC, (b) effect of fibre-orientation on surface roughness, and (c) effect of fibre-orientation on subsurface damage.

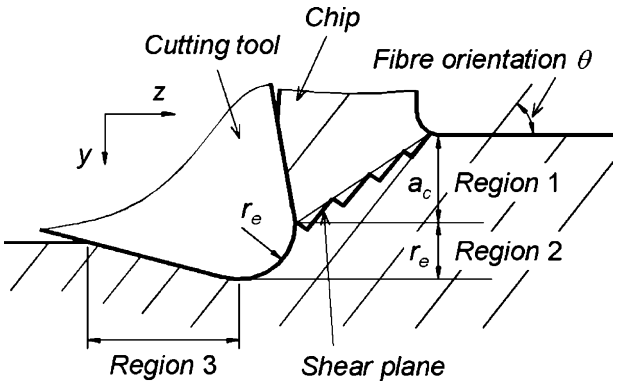

Fig. 2. Deformation zones when cutting an LFRC.

the fibre-matrix interface debonding in the fibre-axis direction. The second distinct deformation region takes place under the nose of the cutting tool, where the nose pushes down the workpiece material. For convenience, it is called the *Pressing Region* or *Region 2*. The third region, called the *Bouncing Region* or *Region 3*, involves mainly the bouncing back of the workpiece material, which happens under the clearance face of the cutting tool. When the fibre-orientation is beyond 90°, more deformation mechanisms take place. As shown in Fig. 1(c), in this case both the fibre–matrix debonding and fibre bending contribute significantly to the deformation and material removal.

2.2. Model derivation

In the following we will discuss the case of $\theta \leq 90^\circ$ only. Based on the above understanding, we know that a mechanics model of cutting must reflect the deformation mechanisms, suggesting that the cutting zone in the model should be also divided to three distinct regions. Region 1 has a depth of a_c, as illustrated in Figs. 2 and 3, bounded by the starting point of the tool nose according to the experiment. Region 2 covers the whole domain under the tool nose, as indicated in Fig. 4, having a depth equal to the nose radius, r_e. Region 3 starts from the lowest point of the tool, as shown in Fig. 5. As a first approximation, it is acceptable to assume that the total cutting force can be calculated by adding up the forces in all the three regions. For convenience, the positive directions of the forces are taken to be in the positive y- and z-directions as defined in Fig. 2.

The above analysis enables us to work out the total cutting forces in vertical and horizontal directions, F_y and F_z, as

$$\begin{cases} F_y = F_{y1} + F_{y2} + F_{y3} \\ F_z = F_{z1} + F_{z2} + F_{z3} \end{cases}$$

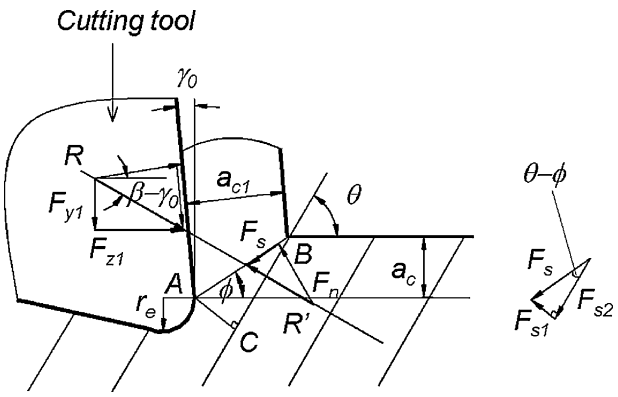

Fig. 3. Forces in Region 1.

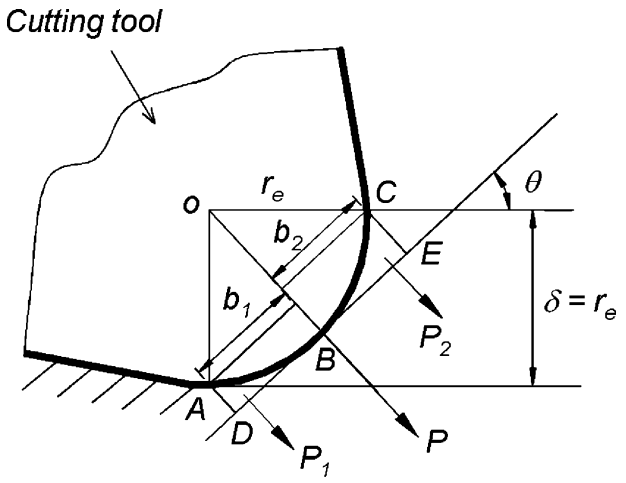

Fig. 4. Forces in Region 2.

where F_{yi} and F_{zi} ($i = 1, 2, 3$) are the corresponding forces in Regions 1–3, defined by

$$\begin{cases} F_{z1} = \tau_1 h a_c \dfrac{\sin\phi\tan(\phi+\beta-\gamma_0)+\cos\phi}{(\tau_1/\tau_2)\cos(\theta-\phi)\sin\theta-\sin(\theta-\phi)\cos\theta} \\ F_{y1} = \tau_1 h a_c \dfrac{\cos\phi\tan(\phi+\beta-\gamma_0)-\sin\phi}{(\tau_1/\tau_2)\cos(\theta-\phi)\sin\theta-\sin(\theta-\phi)\cos\theta} \end{cases}$$

$$\begin{cases} F_{y2} = P_{\text{real}}(\cos\theta - \mu\sin\theta) \\ F_{z2} = P_{\text{real}}(\sin\theta + \mu\cos\theta) \end{cases}$$

$$\begin{cases} F_{y3} = \dfrac{1}{2} r_e E_3 h(1-\mu\cos\alpha\,\sin\alpha) \\ F_{z3} = \dfrac{1}{2} r_e E_3 h\cos^2\alpha \end{cases}$$

in which $\phi \approx \arctan\{\cos\gamma_0/(1-\sin\gamma_0)\}$, E_3 is the effective modulus of the workpiece material in Region 3, h is the thickness of the workpiece, r_e is the tool nose radius, ν is the minor Poisson's ratio, $P_{\text{real}} = K{\cdot}P$ is the real resultant force in Region 2 in which the coefficient K is a function of fibre-orientation to be determined by experiment, μ is the friction coefficient, τ_1 and τ_2 are the shear strengths of the material in AC and BC directions in Fig. 4, γ_0 is the rake angle of the tool, and β is the friction angle on the rake face.

2.3. Model verification

We focus on two materials, MTM56 and F593, because Wang and Zhang (1999) have measured experimentally the property parameters and results in terms of cutting forces which are useful for examining the validity of the model. With these materials, we can determine experimentally that $\tau_1 = 90$ MPa, $\tau_2 = 20$ MPa, $\beta = 30^\circ$, $\mu = 0.15$, $E = 10$ GPa, $\nu = 0.026$ and $K = \{\arctan(30/\theta)\}/2$. The specimen thickness is $h = 4$ mm. Fig. 6 shows the comparison between the model predictions and experimental measurements. It can be seen that the model predicts nicely the nature of the cutting force variation when the cutting parameters change. This means that the model has captured the major deformation mechanisms in cutting the LFRCs. Although the maximum error of the predictions is relatively large, ~30%, it is understandable because experimental measurements were influenced by many factors too. For instance, in making the LFRC specimens, it was impossible to align the fibres perfectly in desired orientations or to distribute them uniformly throughout the specimens.

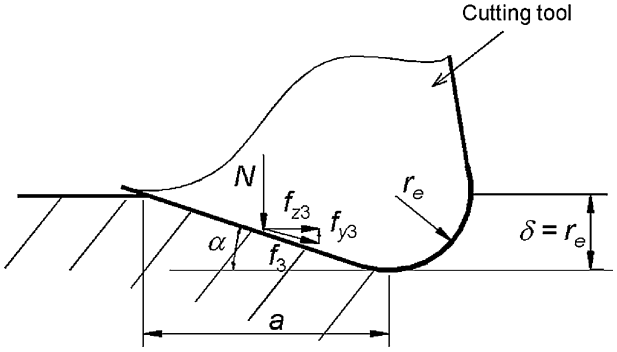

Fig. 5. Forces in Region 3.

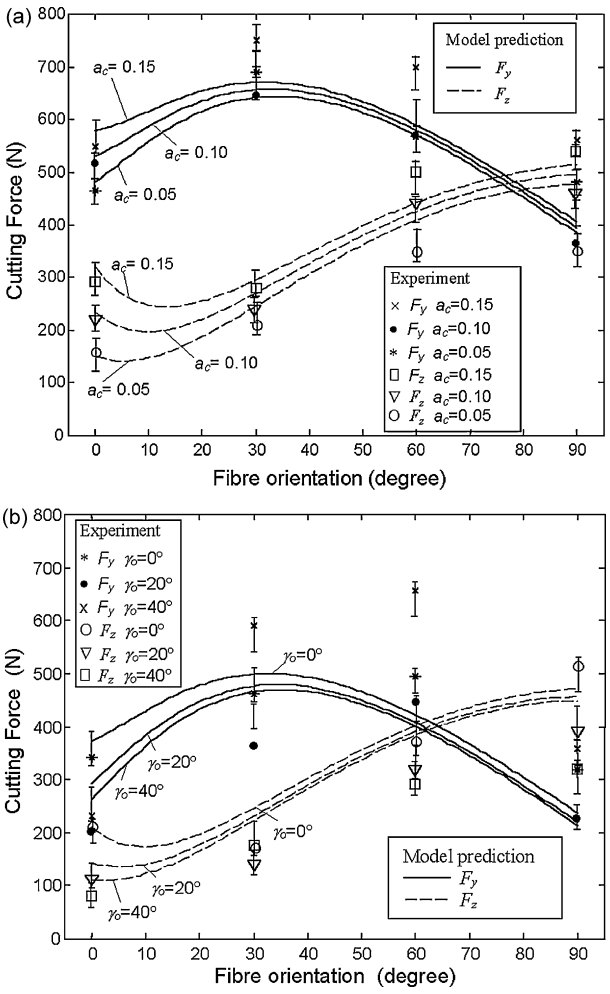

Fig. 6. Cutting forces: model predictions vs. experimental measurements. (a) Variation with depth of cut and fibre-orientation (MTM56, $E_3 = 5.5$ GPa) and (b) variation with rake angle and fibre-orientation (F593, $E_3 = 3.5$ GPa).

3. Cutting of MMCs

3.1. Mechanism understanding

Since MMCs contain ceramic particles, their machining forces depend on the matrix, the reinforcement and their interactions. Lin et al. (1998), El-Gallab and Sklad (1998) and Karthikeyan et al. (2001) carried out some machining tests on aluminium alloy-based MMCs. They found that sharp tools produce continuous chips, but worn tools or cutting at higher depths/feeds develop semi-continuous chips. This means that the type of chips in machining MMCs changes with the cutting conditions and/or tool conditions.

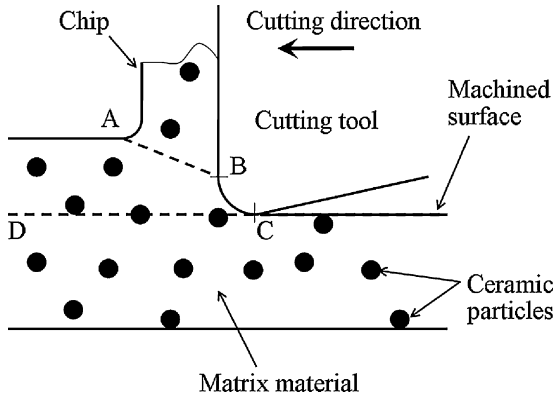

Fig. 7. Cutting of an MMC.

Hung et al. (1998) found that although cracks have been observed at the root of chips, there are similarities in the chip formation mechanism of MMCs to that of monolithic materials. For example, the flow lines formed (El-Gallab and Sklad, 1998; Hung et al., 1999) with particles in the MMCs are similar to those due to the deformation of grain boundaries, etched patterns in steel, aluminium, titanium or brass (Hung et al., 1998). In the chip root region, Hung et al. (1999) observed that these ceramic particles were aligned along a shear plane. On the other hand, the existence of fractured and displaced particles on the machined surface observed by Pramanik et al. (2006), El-Gallab and Sklad (1998) and Hung et al. (1999) indicates that particle fracture and displacement play an important role in machining MMCs. Moreover, in an investigation of a single point scratching of four different aluminium alloy-based MMCs, Yan and Zhang (1995) found that the scratching process involves rubbing, ploughing, plastic cutting and particle fracture.

The above discussion indicates that chip formation, ploughing, and particle fracture/displacement are the major factors in determining cutting forces of an MMC.

3.2. Model derivation

A typical orthogonal cutting process of an MMC is shown in Fig. 7. Based on the mechanism understanding achieved above, we can assume that the chip formation is due to shearing at the shear plane AB. Because of this assumption, the chip formation becomes similar to the orthogonal cutting of a monolithic material with a sharp tool.

The process of ploughing occurs due to the material deformation and displacement by the rounded part of the cutting edge (BC in Fig. 7). This is the plastic deformation zone where no chip is formed. In addition to ploughing, particle fracture and displacement also take place in this region. According to experimental observations by Yan and Zhang (1995), the particle fracture and displacement occur mainly along the cutting line CD (Fig. 7).

Now we can use a similar modelling process to that of cutting LFRCs discussed in the last section. Again, as a first approximation, we can assume that the total cutting force is the superposition of the individual force contributions from chip formation, ploughing and particle fracture/displacement. In chip formation, the forces can be determined by the Merchant's analysis (Merchant, 1945); the forces by ploughing deformation in the metal matrix can be worked out by the slip-line field theory (Waldorf, 2004); and the forces due to particle fracture/displacement can be solved by fracture mechanics (Pramanik et al., 2006). Hence, the total force in the direction of cutting, F_c, and that in the direction of feed (thrust), F_t, can be derived as

$$\begin{cases} F_c = F_{cc} + F_{cp} + F_{cf} \\ F_t = F_{tc} + F_{tp} + F_{tf} \end{cases}$$

where F_{cc} and F_{tc} are the forces due to chip formation, F_{cp} and F_{tp} are the contributions of ploughing deformation of matrix, and F_{cf} and F_{tf} are caused by particle fracture/displacement. These force components can be derived as

$$\begin{cases} F_{cc} = \tau_s A_c \dfrac{\cos(\beta-\gamma)}{\sin\phi\,\cos(\phi+\beta-\gamma)} \\ F_{tc} = \tau_s A_c \dfrac{\cos(\beta-\gamma)}{\sin\phi\,\cos(\phi+\beta-\gamma)} \end{cases}$$

$$\begin{cases} F_{cp} = \tau_{sm} l r_n \tan\left(\dfrac{\pi}{4}+\dfrac{\gamma}{2}\right) \\ F_{tp} = \tau_{sm} l r_n \left[1+\dfrac{\pi}{2}\right] \tan\left(\dfrac{\pi}{4}+\dfrac{\gamma}{2}\right) \end{cases}$$

$$F_{tf} = F_{cf} = \left(\frac{\mu_g l}{L}\right)\tan\delta.$$

In the above equations, A_c is the cross-sectional area of cut, τ_s is the shear strength of the MMC, β is the mean friction angle, γ is the tool rake angle, ϕ is the shear angle defined by $\tan\phi = r_c\cos\gamma/(1-r_c\sin\gamma)$, r_c is chip thickness ratio (ratio of cut-thickness to chip thickness), r_n is the cutting edge radius, τ_{sm} is the shear strength of the matrix material, δ is the angle of resultant force measured from the cutting direction, L is the cutting distance, μ_g is the average fracture energy per unit cutting edge length, and l is the active cutting edge length given by

$$l = r_\varepsilon\left[\kappa_r + \arcsin\left(\frac{f}{2r_\varepsilon}\right)\right] + \frac{a - r_\varepsilon[1-\cos(\kappa_r)]}{\sin(\kappa_r)}$$

where r_ε is the tool nose radius, κ_r is the approach angle, f is the feed and a is the depth of cut.

3.3. Model verification

To verify the model, we conducted a dry turning experiment on a lathe, Mori-Seiki MT2000α1sz. The MMC used was 6061

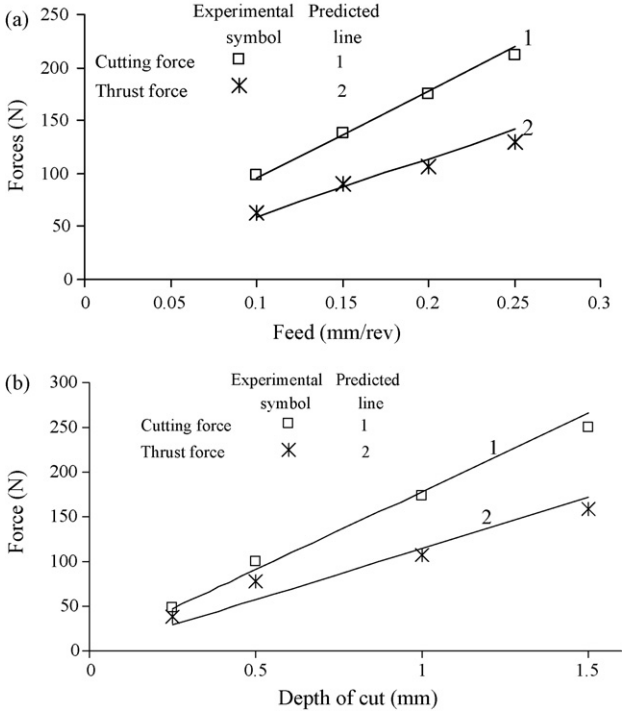

Fig. 8. Model prediction vs. experimental measurement. (a) Effect of feed and (b) effect of depth of cut.

aluminium matrix reinforced by 20 vol% SiC particles of size 6–18 μm (labeled as F3S.20S by Alcan). The cutting tool was polycrystalline diamond (CTH025 of Element-6) tipped TPMN 160304 inserts with its nose radius 0.4 mm, rake angle 5°, approach angle 90°, and cutting edge (without edge hone) radius 5.42 μm.

Fig. 8 compares the theoretically predicted and the experimentally measured forces with varying feed and depth of cut. It is clear that the model predicts extremely well the experimental measurements.

4. Discussion and concluding remarks

We can see from the above examples that the establishment of the models has a common process of mechanism understanding, model derivation, and model verification. These are critical steps.

Mechanism understanding is central because the material removal process of a composite during machining involves significant complexity. It is this step that enables us to get rid of the minor factors, so that we are able to simplify our model without losing the main, essential deformation characteristics such that the model will reliably reflect the major mechanisms of cutting.

Model derivation is associated with a comprehensive application of mechanics theories. In machining, we often have plenty of theories to use, such as contact mechanics, fracture mechanics, elasticity and plasticity. Since our aim is to obtain a model with a manageable degree of formulation for direct applications, it is sensible to use some simplified theoretical tools whenever possible, such as the method of slip-line field for plastic deformation analysis.

The validity and applicability of a model must be well established. In the examples above, experimental measurements have been the tool to demonstrate the predictability of the models and their accuracy. If a model's prediction does not align well with experimental measurements, it is likely that some factors that play important roles have been overlooked in the mechanism understanding and model derivation.

Acknowledgement

The author wishes to thank the Australian Research Council for financial assistance.

References

Arola, D., Ramulu, M., 1997. Orthogonal cutting of fiber-reinforced composites: a finite element analysis. International Journal of Mechanical Science 39, 597–613.
Bhatnagar, N., Ramakrishnan, N., Naik, N.K., Komanduri, R., 1995. On the machining of fiber reinforced plastic (FRP) composite laminates. International Journal of Machine Tools and Manufacture 35, 701–716.
El-Gallab, M., Sklad, S., 1998. Machining of Al/SiC particulate metal matrix composites Part II: work surface integrity. Journal of Material Processing Technology 83, 277–285.
Hung, N.P., Loh, N.L., Venkatesh, V.C., 1999. Machining of metal matrix composites. In: Jahanmir, S., Ramulu, M., Koshy, P. (Eds.), Machining of Ceramics and Composites. Marcel Dekker Inc., New York, pp. 295–356.
Hung, N.P., Yeo, S.H., Lee, K., Ng, K.J., 1998. Chip formation in machining particle-reinforced metal matrix composites. Materials and Manufacturing Processes 13, 85–100.
Karthikeyan, R., Ganesan, G., Nagarazan, R.S., Pai, B.C., 2001. A critical study on machining of Al/SiC composites. Materials and Manufacturing Processes 16, 47–60.
Kishawy, H.A., Kannan, S., Balazinski, M., 2004. An energy based analytical force model for orthogonal cutting of metal matrix composites. Annals of the CIRP 53, 91–94.
König, W., Wulf, Ch., Graβ, P., Willerscheid, H., 1985. Machining of fibre reinforced plastics. Annals of the CIRP 34, 537–548.
Lin, J.T., Bhattacharyya, D., Ferguson, W.G., 1998. Chip formation in the machining of SiC-particle-reinforced aluminum–matrix composites. Composites Science and Technology 58, 285–291.
Mahdi, M., Zhang, L.C., 2001. A finite element model for the orthogonal cutting of fibre-reinforced composite materials. Journal of Materials Processing Technology 113, 373–376.
Merchant, M.E., 1945. Mechanics of the metal cutting process. I. Orthogonal cutting and type 2 chip. Journal of Applied Physics 16, 267–275.
Pramanik, A., Zhang, L.C., Arsecularatne, J.A., 2006. Prediction of cutting forces in machining of metal matrix composites. International Journal of Machine Tools and Manufacture 46, 1795–1803.
Waldorf, D.J., 2004. A simplified model for ploughing forces in turning. Transaction of NAMRI of SME 32, 447–454.
Wang, D.H., Ramulu, M., Arola, D., 1995. Orthogonal cutting mechanisms of graphite/epoxy composite. Part I: unidirectional laminate. International Journal of Machine Tools and Manufacture 35, 1623–1638.
Wang, X.M., Zhang, L.C., 1999. Machining damage in unidirectional fibre-reinforced plastics. In: Wang, J., Scott, W., Zhang, L.C. (Eds.), Abrasive Technology—Current Development and Applications. World Scientific, Singapore, pp. 429–436.
Yan, C., Zhang, L.C., 1995. Single-point scratching of 6061 Al alloy reinforced by different ceramic particles. Applied Composite Materials 1, 431–447.
Zhang, H.J., Chen, W.Y., Chen, D.C., Zhang, L.C., 2001a. Assessment of the exit defects in carbon fibre-reinforced plastic plates caused by drilling. Key Engineering Materials 196, 43–52.
Zhang, L.C., Zhang, H.J., Wang, X.M., 2001b. A new mechanics model for predicting the forces of cutting unidirectional fibre-reinforced composites. Machining Science and Technology 5, 293–305.